Research Article

Thermoelastic analysis of semiconducting solid sphere based on modified Moore-Gibson-Thompson heat conduction with Hall Effect

Iqbal Kaur[1] · Kulvinder Singh[2]

Abstract

The main contribution of this study is to present a unique new mathematical model of photo-thermoelastic interactions with Hall current effect in an infinite semiconducting solid sphere due to high magnetic field acting along its axis. A variable heat flux is applied to the boundary surface of a solid semiconductor sphere. A generalized modified Moore-Gibson-Thompson-Photo-Thermal (MGTPT) theory is used to express the governing equations. In the Green Nagdhi (GN III) model, a thermal relaxation parameter and carrier density parameter is introduced to obtain the new modified Moore-Gibson-Thompson equation (MGT). This mathematical model is solved using Laplace's transforms. Various components of displacement, thermodynamic temperature, conductive temperature, carrier density and axial stress as well as couple stress are obtained in the transformed domain. To get the solution in physical domain, numerical inversion techniques have been employed. The effect various thermoelasticity theories and Hall current is shown graphically on the physical quantities.

Article highlights

- A novel mathematical model of semiconducting solid sphere under a high magnetic field is presented.
- The medium is exposed to variable heat flux at its boundary surface.
- Dynamic response of Moore-Gibson-Thompson-Photo-Thermal theory and Hall Effect is investigated.
- The effects of Hall Effect and various model of thermoelasticity on all physical fields are studied and illustrated graphically.

Abbreviations

δ_{ij}	Kronecker delta
β_{ij}	Thermal elastic coupling tensor
T	Thermodynamic temperature
T_0	Reference temperature s.t. $\left\|T/T_0\right\| << 1$
N_0	Carrier concentration at equilibrium position
F_r	Radial component of Lorentz force
τ_0	Thermal relaxation parameter
ω_e	Electron frequency
D_e	Carrier diffusion coefficients
H_i	Intensity tensor of the magnetic field
α_t	Linear thermal expansion coefficient

✉ Iqbal Kaur, bawahanda@gmail.com; Kulvinder Singh, ksingh2015@kuk.ac.in | [1]Department of Mathematics, Government College for Girls Palwal, Kurukshetra, Haryana, India. [2]UIET, Kurukshetra University, Kurukshetra, Haryana, India.

δ_n	Electronic deformation coefficient
K_{ij}	Coefficient of Thermal conductivity
d_n	Coefficient of electronic deformation
ϵ_{ijk}	Permutation symbol
$H(t)$	Heaviside function
σ_0	Electrical conductivity
n_e	Electron number density
m_e	Electron mass
μ_0	Magnetic permeability
λ, μ	Lame's elastic constants
τ	Photo-generated carrier lifetime
N	Carrier density
ρ	Medium density (kg m^{-3})
e_{kk}	Cubical dilatation
J_i	Conduction current density tensor
E_g	Energy gap of the semiconductor parameter
t	Time
Ω	Angular frequency
F_i	The body force
K_{ij}^*	Material constant
m	Hall Effect parameter
e_{ij}	Strain tensors (mm^{-1})
κ	Coupling parameter for thermal activation
H_0	Magnetic field
u_i	Components of displacement (m)
s_v	Surface recombination velocity
c_e	Electron charge
t_e	Electron collision time
E_i	Intensity tensor of the electric field
C_e	Specific heat at constant strain
σ_{ij}	Stress tensors (N m^{-2})

1 Introduction

With the advancement of the technology, the size of the components of Microelectronic devices is continuously reducing. More and more components are fabricated on the small semiconducting crystal chip. By using a sphere-shaped semiconductor integrated circuit, it is possible to utilize the semiconductor material (SM) more efficiently. A semiconductor with a spherical shape provides more surface area for a circuit to be fabricated. Semiconductor spheres could reduce the cost of manufacturing integrated circuits by 90% by replacing clean rooms with hermetically sealed tubes and by reducing the processing cycle time from months to days. Microprocessor manufacturers have invested on large scale in the production of large silicon crystals. When a semiconductor crystal is irradiated with an excitation laser, standard approaches can be used to determine the amount of light it emits. SM contribution to technological advancement was recently demonstrated when

they were used to generate electrical energy from sunlight, even when irradiated to laser light. SM are used to fabricate the solar cell to generate the alternative energy sources. Moreover, in the field of electronics and electrical engineering, SM have been used for nanomaterials. In the current industry, they can be used for a variety of things, such as VLSI, solar cells, etc. The resemblance between thermoelasticity and photothermal equations has been described using numerous mathematical models.

A growing interest in semiconductor nanostructures has been observed among researchers working in nanotechnology. Further, it is impossible to fully investigate semiconducting micro/nano-devices without studying the thermoelasticity, as according to thermoelasticity, the SM can be classified as elastic materials. A number of theoretical models have been examined to determine how photothermal equations relate to thermoelasticity. The classical uncoupled thermoelasticity theory was introduced by Duhamel [1]. Two limitations are associated with this theory. Firstly, the state of elastic materials is independent of temperature. Furthermore, as a consequence of the parabolic heat equation, it expects that temperature travels at an infinite speed, again in conflict with physical experimentation. Biot [2] gave coupled thermoelasticity as a solution to these problems. This theory relates equations of heat conduction to elasticity equations. Despite this, this theory only predicts heat waves propagating at an unlimited speed. When a temperature gradient is abruptly imposed on a homogeneous and isotropic medium, Cattaneo [3] and Vernotte [4, 5] propose a broader form of Fourier law that incorporates a relaxation time to define a steady state, as follows:

$$\left(1 + \tau_0 \frac{\partial}{\partial t}\right)\boldsymbol{q} = -K_{ij}\nabla\mathbf{T}, \qquad (1)$$

Lord and Shulman [6] then presented a generalized theory of thermoelasticity with one relaxation time for an isotropic body. The heat equation is hyperbolic in this theory, therefore, temperature propagates at a finite speed. Subsequent, Green and Lindsay [7] gave a more accurate interpretation of thermoelasticity that demonstrated the linear heat conduction tensor symmetry. Dhaliwal and Sherif [8] gave the comprehensive thermoelasticity equations for an anisotropic medium, Conversely, Green and Naghdi [9–11] introduced "the linear and the nonlinear thermoelastic theories with and without energy dissipation" and expanded the Fourier law as

$$q = -K_{ij}\nabla T - K_{ij}^*\nabla\vartheta, \dot{\vartheta} = T. \qquad (2)$$

Based on entropy equality, they proposed three new thermoelastic theories. Their theories are known as

the thermoelasticity theory of type I, the thermoelasticity theory of type II (i.e., thermoelasticity without energy dissipation), and the thermoelasticity theory of type III (i.e., thermoelasticity with energy dissipation). On linearization, type I becomes the classical heat equation whereas on linearization type-II, as well as type-III theories, give the finite speed of thermal wave propagation.

In recent years, numerous academic works has been carried out to analyze and explain the MGT equation. A 3rd-order differential equation that is vital to several fluid dynamics is the basis of Lasiecka and Wang [12] theory. Quintanilla [13, 14] created a unique heat conduction model using the MGT equation with 2 T. The MGT theory states that the modified Fourier law as

$$\left(1 + \tau_0 \frac{\partial}{\partial t}\right) q = -K_{ij} \nabla \mathrm{T} - K_{ij}^* \nabla \vartheta, \quad \text{where } \dot{\vartheta} = T. \tag{3}$$

Linear thermoelastic deformations of dielectrics were explored by Fernandez and Quintanilla [15]. Assume that a SM is irradiated to an external laser beam, which causes excited free electrons with semiconductor gap energy E_g to form a carrier-free charge density. Electronic distortion and elastic vibration change as a result of optical energy absorption. In this occurrence, thermal-elastic-plasma waves will have an impact on heat conductivity equations. The expanded definition of the modified Fourier law for SM with plasma impact is as follows:

$$\left(1 + \tau_0 \frac{\partial}{\partial t}\right) q = -K_{ij} \nabla T - K_{ij}^* \nabla \vartheta - \int \frac{E_g N}{\tau} dx, \quad \text{where } \dot{\vartheta} = T. \tag{4}$$

By differentiating the Eq. (4) w.r.t. $\bar{x}$, yields

$$\left(1 + \tau_0 \frac{\partial}{\partial t}\right) \nabla . q = -\nabla . \left(K_{ij} \nabla T + K_{ij}^* \nabla \vartheta\right) - \frac{E_g N}{\tau}, \quad \text{where } \dot{\vartheta} = T. \tag{5}$$

Kaur et al. [16] examined the semi-conducting solid cylinder exposed to exponential laser pulse with MGTPT and Hall current effect. In addition to these, Gupta et al. [17–19], Craciun et al. [20, 21], Kaur and Singh [22, 23], Kaur et al. [24], Tiwari and Mukhopadhyay [25], Kaur et al. [26], Tiwari et al. [27, 28], Marin et al. [29], Gupta et al. [30, 31], Kumar et al. [32] also done studies on the Hall current effect and other theories of thermoelasticity. The literature survey revealed, however, that no research had been done on the transient examination of a semiconductor sphere exposed to ultrashort pulsed laser heating and photogenerated plasma under the Hall Effect.

In this research, we have undertaken transient examination of a semiconductor sphere exposed to ultrashort pulsed laser heating and photogenerated plasma under the Hall Effect. The basic equations of semiconducting solid sphere are expressed with MGTPT heat transfer theory using GN III model. The Sect. 1 illustrated the evolution of the Fourier's Law and the heat conduction equation. The Sect. 2 focuses on the basic equation for semiconducting medium viz equation of motion, equation of the plasma diffusion and MGTPT. Section 3 describe the mathematical formulation of the study of semiconductor solid sphere with MGTPT heat transfer equation to obtain the dimensionless expressions for Various components of displacement, thermodynamic temperature, conductive temperature, carrier density and axial stress as well as couple stress are found in the transformed domain using Laplace Transforms. Boundary conditions for sphere's exterior surface constrained by time dependent variable heat has been discussed in the Sect. 4. The Sects. 5 and 6 provide the solution to problem and method for the Laplace Transform inversion. The Sect. 7 presents the numerical results and shows the effect of various thermoelasticity theories and Hall current on the physical quantities graphically with MATLAB software. The Sect. 8 deals with the conclusions of the paper.

2 Basic equations

Following Mahdy et al. [33], Abouelregal and Atta [34], the governing equations for a photo-magneto-thermoelastic with new modified green Nagdhi model is given by.

Constitutive relations

$$\sigma_{ij} = \left(\lambda u_{k,k} - \beta T - \delta_n N\right) \delta_{ij} + \mu\left(u_{i,j} + u_{j,i}\right), \tag{6}$$

$$\beta = (3\lambda + 2\mu)\alpha_t, \delta_n = (3\lambda + 2\mu)d_n.$$

Equation of motion

$$\sigma_{ij,j} + F_i = \rho \ddot{u}_i, \tag{7}$$

Plasma diffusion equation

$$\frac{\partial \boldsymbol{N}}{\partial t} = D_E \nabla^2 N - \frac{N}{\tau} + \kappa T, \tag{8}$$

where $\kappa = \frac{T}{\tau} \frac{\partial N_0}{\partial T}$.

Modified Moore Gibson Thompson photo thermal equation

$$\left(K_{ij} \dot{T}_{,j}\right)_{,i} + \left(K_{ij}^* T_{,j}\right)_{,i} + \frac{E_g \dot{N}}{\tau} = \left(1 + \tau_0 \frac{\partial}{\partial t}\right) \left[\rho C_E \ddot{T} + \beta_{ij} T_0 \ddot{e}_{ij} - \rho \dot{Q}\right], \tag{9}$$

where $K_{ij} = K_i \delta_{ij}, K_{ij}^* = K_i^* \delta_{ij}, i$ is not summed.

Improved Ohm's law with Hall effect

$$J_i = \sigma_0 \left(E_i + \mu_0 \epsilon_{ijr} \left(u_{j,t} - \frac{\mu_0}{en_e} J_j \right) H_r \right). \tag{10}$$

where $\sigma_0 = \frac{n_e e^2 t_e}{m_e}, m = \omega_e t_e = \frac{\sigma_0 \mu_0 H_0}{en_e}, \omega_e = \frac{e\mu_0 H_0}{m_e}$.

Vector form of Eq. (8) is

$$J = \sigma_0 \left\{ E + \mu_0 (\dot{u} \times H) - \frac{\mu_0}{en_e} (J \times H) \right\}.$$

Lorentz force

$$F_i = \mu_0 \epsilon_{ijk} J_j H_k, \tag{11}$$

Here, the subscript followed by "," comma denotes partial derivative w.r.t. respective space variable and a superposed dot represents derivative w.r.t. time variable t.

where $\epsilon_{ijk} = \epsilon_{jki} = \epsilon_{kij} = -\epsilon_{jik} = -\epsilon_{kji} = -\epsilon_{ikj}$,

$$\epsilon_{ijk} = \begin{cases} +1, & \text{if } (i,j,k) \text{ is even permutation of } (1,2,3), \\ -1, & \text{if } (i,j,k) \text{ is odd permutation of } (1,2,3), \\ 0, & \text{if two or more indices are equal.} \end{cases}$$

$(i.e. \epsilon_{123} = +1, \epsilon_{132} = -1, \epsilon_{122} = 0).$

3 Mathematical model of the problem

Consider a thermally homogenous, infinitesimal semiconductor solid sphere of radius R (Fig. 1) where the outer surface is traction-free and a time-dependent
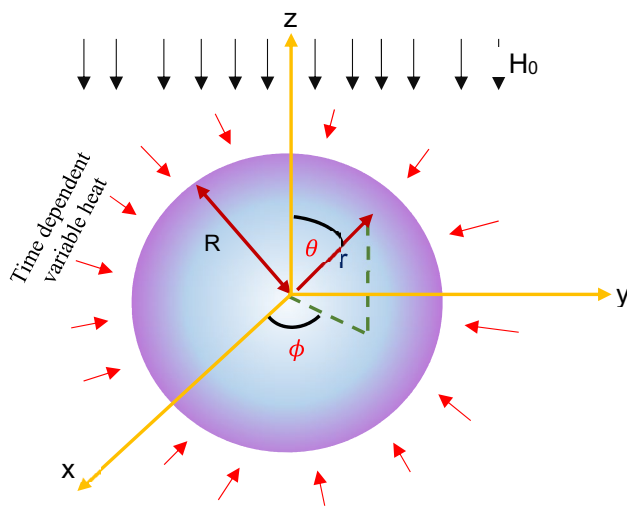

Fig. 1 Schematic diagram of semiconducting solid sphere

variable heat flux is applied to it. No heat sources exist inside the sphere. The spherical coordinate system (r, θ, ϕ) are considered to model the problem with $(0 \leq r \leq R), (0 \leq \theta \leq 2\pi), (0 \leq \phi \leq 2\pi)$. Initially, the sphere is kept at constant and uniform temperature (T_0).

For 1D problem, displacement components and the displacement–strain relations which depends on radial distance r and the time t due to symmetry are given by

$$u = \left(u_\rho, u_\theta, u_\phi \right) = (u, 0, 0)(r, t), \tag{12}$$

$$e_{rr} = \frac{\partial u}{\partial r}, e_{\theta\theta} = e_{\phi\phi} = \frac{u}{r}, e_{r\theta} = e_{r\phi} = e_{\theta\phi} = 0. \tag{13}$$

The dilatation term e is given by

$$e = \frac{1}{r^2} \frac{\partial (r^2 u)}{\partial r}. \tag{14}$$

The Eq. (6) using (12) and (13) yields

$$\sigma_{rr} = (\lambda + 2\mu) + 2\lambda \frac{u}{r} - (\beta T + \delta_n N), \tag{15}$$

$$\sigma_{\theta\theta} = \sigma_{\phi\phi} = \lambda \frac{\partial u}{\partial r} + 2(\lambda + \mu) \frac{u}{r} - (\beta T + \delta_n N), \tag{16}$$

The dynamic equation of motion using the Lorentz force, turn into

$$\frac{\partial \sigma_{rr}}{\partial r} + \frac{1}{r} \left(2\sigma_{rr} - \sigma_{\theta\theta} - \sigma_{\phi\phi} \right) + F_r = \rho \frac{\partial^2 u}{\partial t^2}. \tag{17}$$

Assume that the sphere is under a constant and extremely strong magnetic field $\boldsymbol{H}_0 = (0, 0, H_0)$, in addition, assume that $\boldsymbol{E} = 0$. Under these conventions from the generalized Ohm's law (8) we have.

$$J_\phi = 0. \tag{18}$$

Accordingly the components of current density J_r and J_θ are given as

$$J_r = \frac{\sigma_0 \mu_0 H_0}{1 + m^2} \left(m \frac{\partial u}{\partial t} \right), \tag{19}$$

$$J_\theta = \frac{\sigma_0 \mu_0 H_0}{1 + m^2} \left(-\frac{\partial u}{\partial t} \right). \tag{20}$$

F_r induced by $\boldsymbol{H}_0$ is given by

$$F_r = \mu_0 (\boldsymbol{J} \times \boldsymbol{H})_r. \tag{21}$$

Using Eqs. (15, 16 and 18–21) in Eqs. (17) and also from (8, 9) in spherical coordinates, the governing equations for the semiconducting solid sphere are:

$$(\lambda + 2\mu)\frac{\partial e}{\partial r} - \beta\frac{\partial T}{\partial r} - \delta_n\frac{\partial N}{\partial r} - \frac{\sigma_0\mu_0^2 H_0^2}{1+m^2}\left(\frac{\partial u}{\partial t}\right) = \rho\frac{\partial^2 u}{\partial t^2}, \quad (22)$$

$$\frac{\partial N}{\partial t} = D_E\left(\nabla^2 N\right) - \frac{N}{\tau} + \kappa T, \quad (23)$$

$$K\frac{\partial}{\partial t}\nabla^2 T + K^*\nabla^2 T + \frac{E_g\dot{N}}{\tau} = \left(1 + \tau_0\frac{\partial}{\partial t}\right)\left[\rho C_E\frac{\partial^2 T}{\partial t^2} + \beta T_0\frac{\partial^2 e}{\partial t^2}\right]. \quad (24)$$

In the spherical coordinate system, the Laplacian operator ∇^2, is given by.

$$\nabla^2 = \frac{\partial^2}{\partial r^2} + \frac{2}{r}\frac{\partial}{\partial r} = \frac{1}{r^2}\frac{\partial}{\partial r}\left(r^2\frac{\partial}{\partial r}\right). \quad (25)$$

Pre-operating both sides of Eq. (22) by $\left(\frac{2}{r} + \frac{\partial}{\partial r}\right)$, yields

$$(\lambda + 2\mu)\nabla^2 e - \beta\nabla^2 T - \delta_n\nabla^2 N - \frac{\sigma_0\mu_0^2 H_0^2}{1+m^2}\left(\frac{\partial e}{\partial t}\right) = \left(\frac{\partial^2 e}{\partial t^2}\right). \quad (26)$$

The following dimensionless quantities are used to find the dimensionless form of above equations:

$$(r', u') = v_0\eta(r, u), \left(T', N', \sigma'_{ij}\right) = \frac{1}{\rho v_0^2}\left(\beta T, \delta_n N, \sigma_{ij}\right), (\tau'_0, \tau', t') = v_0^2\eta(\tau_0, \tau, t), \eta = \frac{\rho C_E}{K}, \rho v_0^2 = \lambda + 2\mu, M = \frac{\sigma_0\mu_0^2 H_0^2}{\eta\rho v_0^2}, \gamma = \sqrt{\frac{2\mu}{\lambda + 2\mu}}. \quad (27)$$

M is the Hartmann number or magnetic parameter in semiconductor elastic medium and it measures the magnetic field strength. Using the dimensionless quantities (27) in Eqs. (24, 25 and 26), and after suppressing the primes, yields

$$\nabla^2 e - \nabla^2 T - \nabla^2 N - \frac{M}{1+m^2}\left(\frac{\partial e}{\partial t}\right) = \left(\frac{\partial^2 e}{\partial t^2}\right), \quad (28)$$

$$\frac{\partial N}{\partial t} = \delta_1\left(\nabla^2 N\right) - \delta_2 N + \delta_3 T, \quad (29)$$

$$\frac{\partial}{\partial t}\nabla^2 T + \delta_4\nabla^2 T + \delta_5 N = \left(1 + \tau_0\frac{\partial}{\partial t}\right)\left[\frac{\partial^2 T}{\partial t^2} + \delta_6\frac{\partial^2 e}{\partial t^2}\right], \quad (30)$$

where

$$\sigma_{rr} = \gamma^2\frac{\partial u}{\partial r} + \left(1 - \gamma^2\right)e - (T + N), \quad (31)$$

$$\sigma_{\theta\theta} = \sigma_{\phi\phi} = \gamma^2\frac{u}{r} + \left(1 - \gamma^2\right)e - (T + N), \quad (32)$$

The preliminary conditions of this model are

$$u(r, 0) = 0 = \frac{\partial u}{\partial t}(r, 0), \quad (33)$$

$$T(r, 0) = 0 = \frac{\partial T}{\partial t}(r, 0), \quad (34)$$

$$N(r, 0) = 0 = \frac{\partial N}{\partial t}(r, 0). \quad (35)$$

The Laplace transform of a function f w.r.t. time variable t, is defined as

$$\mathcal{L}(f(t)) = \bar{f}(s) = \int_0^\infty f(t)e^{-st}dt, \quad (36)$$

where s as a Laplace Transform variable. Applying trans-form defined by (36) to Eqs. (28–32) yields

$$\left(\nabla^2 + \left(-s^2\right) - \frac{Ms}{1+m^2}\right)\bar{e} - \nabla^2\bar{T} - \nabla^2\bar{N} = 0, \quad (37)$$

$$\left(\delta_1\nabla^2 - \left(\delta_2 + s\right)\right)\bar{N} + \delta_3\bar{T} = 0, \quad (38)$$

$$\left(1 + \tau_0 s\right)\delta_6 s^2\bar{e} + \left(-\left(s + \delta_4\right)\nabla^2 + \left(1 + \tau_0 s\right)s^2\right)\bar{T} - \delta_5 s\bar{N} = 0, \quad (39)$$

$$\bar{\sigma}_{rr} = \gamma^2\frac{\partial\bar{u}}{\partial r} + \left(1 - \gamma^2\right)\bar{e} - \left(\bar{T} + \bar{N}\right), \quad (40)$$

$$\bar{\sigma}_{\theta\theta} = \gamma^2\frac{\bar{u}}{r} + \left(1 - \gamma^2\right)\bar{e} - \left(\bar{T} + \bar{N}\right), \quad (41)$$

When Eqs. (37) to (39) are decoupled, we obtain

$$\delta_1 = D_E\eta, \delta_2 = \frac{1}{\tau}, \delta_3 = \frac{\kappa\delta_n}{\beta}, \delta_4 = \frac{K^*}{(\lambda + 2\mu)C_E}, \delta_5 = \frac{E_g}{\delta_n C_E(\lambda + 2\mu)\eta\tau}, \delta_6 = \frac{\beta^2 T_0}{\rho C_E(\lambda + 2\mu)}.$$

By using (27) in Eqs. (15, 16) and after suppressing the primes, yields

$$\left(\nabla^6 - B\nabla^4 + C\nabla^2 - D\right)\left(\bar{e}, \bar{T}, \bar{N}\right) = 0, \quad (42)$$

where $A = -\delta_1\delta_{11}, B = -(A\delta_7 - \delta_1\delta_{10} - \delta_1\delta_9 + \delta_8\delta_{11})/A,$

$C = (-\delta_3\delta_5 s + \delta_3\delta_9 - \delta_1\delta_7\delta_{10} + \delta_8\delta_7\delta_{11} + \delta_8\delta_{10}$
$\quad + \delta_8\delta_9)/A, D = (\delta_3\delta_7\delta_5 s - \delta_8\delta_7\delta_{10})/A,$

$\delta_7 = (-s^2) - \dfrac{Ms}{1 + m^2}, \delta_8 = \delta_2 + s, \delta_9 = (1 + \tau_0 s)\delta_6 s^2,$

$\delta_{10} = (1 + \tau_0 s)s^2, \delta_{11} = -(s + \delta_4).$

Presenting $\lambda_i, i = 1, 2, 3$, in Eqs. (42), we obtain

$$(\nabla^2 - \lambda_1^2)(\nabla^2 - \lambda_2^2)(\nabla^2 - \lambda_3^2)(\overline{e}, \overline{T}, \overline{N}) = 0, \tag{43}$$

where $\lambda_i^2, i = 1, 2, 3$, are the roots of the equation

$$(\lambda^6 - B\lambda^4 + C\lambda^2 - D) = 0, \tag{44}$$

Which are given by

$$\lambda_1^2 = \frac{1}{3}(2d\sin\chi + B),$$

$$\lambda_2^2 = \frac{1}{3}\left\{-d\left(\sin\chi + \sqrt{3}\cos\chi\right) + \frac{B}{3}\right\},$$

$$\lambda_3^2 = \frac{1}{3}\left\{d\left(\sin\chi - \sqrt{3}\cos\chi\right) + \frac{B}{3}\right\},$$

With

$$d = \sqrt{B^2 - 3C}, \chi = \frac{1}{3}\sin^{-1}\left(-\frac{2B^3 - 9BC + 27D}{2d^3}\right).$$

The common solution of (43) can be expressed as follows:

$$(\overline{e}, \overline{T}, \overline{N}) = \frac{1}{\sqrt{r}}\sum_{i=1}^{3}(1, \zeta_i, \eta_i)g_i I_{1/2}(\lambda_i r), \tag{45}$$

where $I_n()$ indicates the second types of modified Bessel functions of order n. We get the following relations by inserting Eq. (45) into Eqs. (37–39)

$$\zeta_i = \frac{-(\lambda_i^2 + \delta_7)(\delta_9\lambda_i^2 - \delta_5)}{\delta_3\delta_5 + (\delta_{11}\lambda_i^2 + \delta_{10})(\delta_1\lambda_i^2 - \delta_8)}, \tag{46}$$

$$\eta_i = \frac{-(\lambda_i^2 + \delta_7)(\delta_3)}{\delta_3\delta_5 + (\delta_{11}\lambda_i^2 + \delta_{10})(\delta_1\lambda_i^2 - \delta_8)}. \tag{47}$$

We have the Bessel function relation

$$\int x^{3/2} I_{1/2}(x)dx = x^{3/2} I_{3/2}(x). \tag{48}$$

In the domain of the Laplace transform, displacement u can be expressed as:

$$\overline{u} = \frac{1}{\sqrt{r}}\sum_{i=1}^{3} g_i \frac{I_{3/2}(\lambda_i r)}{\lambda_i}, \tag{49}$$

The modified Bessel I_n follows the following relationships for any positive number x.

$$I_{1/2}(x) = \sqrt{\frac{2}{\pi x}}\sinh x, \tag{50}$$

$$I_{3/2}(x) = \sqrt{\frac{2}{\pi x}}\left(\cosh x - \frac{\sinh x}{x}\right). \tag{51}$$

Introducing Eq. (50) into Eqs. (45), we obtain

$$(\overline{e}, \overline{T}, \overline{N}) = \sqrt{\frac{2}{\pi}}\sum_{i=1}^{3}(1, \zeta_i, \eta_i)\frac{g_i}{\sqrt{r\lambda_i}}\sinh(\lambda_i r), \tag{52}$$

Using (51) in Eq. (49) the displacement $\overline{u}$ may be represented as follows in the Laplace transform domain:

$$\overline{u} = \sqrt{\frac{2}{\pi}}\sum_{i=1}^{3}\frac{g_i}{r\lambda_i^{3/2}}\left(\cosh(\lambda_i r) - \frac{\sinh(\lambda_i r)}{(\lambda_i r)}\right), \tag{53}$$

Differentiating Eq. (53) in terms of r yields

$$\frac{\partial \overline{u}}{\partial r} = \sqrt{\frac{2}{\pi}}\sum_{i=1}^{3} g_i\{l_i\sinh(\lambda_i r) - n_i\cosh(\lambda_i r)\}. \tag{54}$$

$$l_i = \left(\frac{2 + \lambda_i^2 r^2}{r^3\lambda_i^{5/2}}\right), n_i = \frac{2}{r^2\lambda_i^{3/2}}.$$

Thus, using (52)–(54) in Eqs. (40) and (41), the expressions for thermal stresses are derived as

$$\overline{\sigma_{rr}} = \sqrt{\frac{2}{\pi}}\sum_{i=1}^{3} g_i\{l1_i\sinh(\lambda_i r) - n1_i\cosh(\lambda_i r)\}, \tag{55}$$

$$\overline{\sigma_{\theta\theta}} = \sqrt{\frac{2}{\pi}}\sum_{i=1}^{3} g_i\{p_i\cosh(\lambda_i r) + m_i\sinh(\lambda_i r)\}, \tag{56}$$

$$p_i = \frac{\gamma^2}{r^2\lambda_i^{3/2}}, m_i = \left(\frac{-\gamma^2}{r^{5/2}\lambda_i^2}\right) + \frac{1 - \gamma^2 - (\zeta_i + \eta_i)}{r^{1/2}\lambda_i^{1/2}} \tag{57}$$

$$l1_i = \left(\gamma^2 l_i + \frac{1 - \gamma^2 - (\zeta_i + \eta_i)}{r^{1/2} \lambda_i^{1/2}} \right), n1_i = \gamma^2 n_i.$$

4 Boundary conditions

Assume that the sphere's exterior surface is traction free and is constrained by time dependent variable heat. Hence, the mechanical boundary condition can be expressed as

$$T(R, t) = T_1 H(t), t > 0 \tag{58}$$

$$\sigma_{rr}(R, t) = 0, \tag{59}$$

During the diffusion phase, carriers can reach the sample surface, with a finite probability of recombination. Thus, the carrier density boundary condition is:

$$D_e \frac{\partial N}{\partial r} = s_v N, \text{ at } r = R. \tag{60}$$

By applying the Laplace transform on (58–60) yields

$$\overline{T}(R, s) = \frac{T_0}{s}, \tag{61}$$

$$\tilde{\sigma}_{rr}(R, s) = 0, \tag{62}$$

$$D_e \frac{\partial \overline{N}}{\partial r} \bigg|_{r=r_0} = s_v \overline{N}(r_0, s). \tag{63}$$

Equations (52) and (55) are substituted into Eq. (61–63), giving

$$\sqrt{\frac{2}{\pi}} \sum_{i=1}^{3} g_i \left\{ \frac{\zeta_i}{\sqrt{\lambda_i R}} \sinh(\lambda_i R) \right\} = \frac{T_0}{s}, \tag{64}$$

$$\sum_{i=1}^{3} g_i \{ l1_i \sinh(\lambda_i R) - n1_i \cosh(\lambda_i R) \} = 0, \tag{65}$$

$$\sum_{i=1}^{3} g_i \eta_i \{ a_i \cosh(\lambda_i R) + b_i \sinh(\lambda_i R) \} = 0, \tag{66}$$

$$a_i = \frac{D_E \lambda_i^{1/2}}{R^{1/2}}, b_i = \frac{-D_E}{2R^{3/2} \lambda_i^{3/2}} - \frac{s_v}{\sqrt{\lambda_i R}},$$

$$n_{1i} = \left(\gamma^2 l_{1i} + \frac{1 - \gamma^2 - (\zeta_i + \eta_i)}{R \lambda_i^{1/2}} \right), l_{1i} = \left(\frac{2 + \lambda_i^2 R^2}{R^3 \lambda_i^{5/2}} \right).$$

The values of $g_i, i = 1, 2, 3$ can be obtained by solving Eqs. (64–66) by Cramer's rule

$$g_i(s) = \frac{\Delta_i}{\Delta}, \tag{67}$$

$$\Delta = G_1 [G_5 G_9 - G_8 G_6] - G_2 [G_4 G_9 - G_6 G_7] + G_3 [G_4 G_8 - G_5 G_7],$$

$$\Delta_1 = \frac{T_0}{s} [G_5 G_6 - G_8 G_9],$$

$$\Delta_2 = -\frac{T_0}{s} [G_4 G_9 - G_7 G_6],$$

$$\Delta_3 = \frac{T_0}{s} [G_4 G_8 - G_5 G_7],$$

$$G_i = \sqrt{\frac{2}{\pi}} \left\{ \frac{\zeta_i}{\sqrt{\lambda_i R}} \sinh(\lambda_i R) \right\},$$

$$G_{i+3} = \{ l1_i \sinh(\lambda_i R) - n1_i \cosh(\lambda_i R) \},$$

$$G_{i+6} = \eta_i \{ a_i \cosh(\lambda_i R) + b_i \sinh(\lambda_i R) \}, i = 1, 2, 3$$

And using the values of $g_i(s)$ from Eq. (67) in eqs. (52, 53, 55–56) the different constituents of displacement, temperature distribution, carrier density and stresses are

$$\overline{u} = \frac{1}{\Delta} \frac{T_0}{s} \{ [G_5 G_6 - G_8 G_9] \alpha_1 \\ - [G_4 G_9 - G_7 G_6] \alpha_2 + [G_4 G_8 - G_5 G_7] \alpha_3 \}, \tag{68}$$

$$\overline{T} = \frac{1}{\Delta} \frac{T_0}{s} \{ [G_5 G_6 - G_8 G_9] \zeta_1 \beta_1 \\ - [G_4 G_9 - G_7 G_6] \zeta_2 \beta_2 + [G_4 G_8 - G_5 G_7] \zeta_3 \beta_3 \}, \tag{69}$$

$$\overline{N} = \frac{1}{\Delta} \frac{T_0}{s} \{ [G_5 G_6 - G_8 G_9] \eta_1 \beta_1 \\ - [G_4 G_9 - G_7 G_6] \eta_2 \beta_2 + [G_4 G_8 - G_5 G_7] \eta_3 \beta_3 \}, \tag{70}$$

$$\overline{\sigma}_{rr} = \frac{1}{\Delta} \frac{T_0}{s} \{ [G_5 G_6 - G_8 G_9] \gamma_1 \\ - [G_4 G_9 - G_7 G_6] \gamma_2 + [G_4 G_8 - G_5 G_7] \gamma_3 \}, \tag{71}$$

$$\overline{\sigma_{\theta\theta}} = \frac{1}{\Delta}\frac{T_0}{s}\left\{\left[G_5G_6 - G_8G_9\right]\vartheta_1 \right.$$
$$\left. - \left[G_4G_9 - G_7G_6\right]\vartheta_2 + \left[G_4G_8 - G_5G_7\right]\vartheta_3\right\}, \qquad (72)$$

where

$$\alpha_i = \sqrt{\frac{2}{\pi}}\frac{1}{r\lambda_i^{3/2}}\left(\cosh(\lambda_i r) - \frac{sinh(\lambda_i r)}{(\lambda_i r)}\right), \beta_i = \sqrt{\frac{2}{\pi}}\frac{1}{\sqrt{r\lambda_i}}\sinh(\lambda_i r)$$

$$\gamma_i = \sqrt{\frac{2}{\pi}}\left\{l1_i\sinh(\lambda_i r) - n1_i\cosh(\lambda_i r)\right\}, \vartheta_i$$

$$= \sqrt{\frac{2}{\pi}}\left\{p_i\cosh(\lambda_i r) + m_i\sinh(\lambda_i r)\right\}i = 1, 2, 3.$$

5 Inversion of the transforms

The results in the physical domain problem are obtained by inverting the transforms in Eqs. (68–72) using:

$$f(x, t) = \frac{1}{2\pi i}\int\limits_{e^{-i\infty}}^{e^{+i\infty}}\widetilde{f}(x, s)e^{-st}ds. \qquad (73)$$

Finally evaluate the integral in Eq. (73) using Romberg's integration (Press et al. [35]) with adaptive step size.

6 Particular cases

   i.   If $K^* \neq 0, K \neq 0$ and $\tau_0 \neq 0$ in Eqs. (68–72) the results for the MGTPT can be obtained with Hall Effect.
   ii. If $K^* \neq 0, K \neq 0$ and $\tau_0 = 0$ in Eqs. (68–72) the results for the photothermal Green-Naghdi (PGN) III model can be obtained with Hall Effect
   iii. If $K \neq 0$ and $\tau_0 = 0$ in Eqs. (68–72) the results for the PGN-II can be obtained with Hall Effect.
   iv. If $\tau_0 = 0, K^* = 0$, in Eqs. (68–72), we get the results corresponding to the coupled photo-thermoelasticity theory (CPTE) with Hall Effect.
   v.   If $K^* = 0$, in Eqs. (68–72) we get the results corresponding to the generalized Lord and Shulman photo-thermoelasticity model (PLS) with Hall Effect.

7 Numerical results and discussion

With the MATLAB software the theoretical results are obtained by utilising the following physical data of the silicon (Si) material and the effect of Hall current, and the MGTPT heat equation are illustrated graphically.

$\lambda = 3.64 \times 10^{10}$ Nm^{-2}	$T_0 = 300$ K
$\mu = 5.46 \times 10^{10}$ Nm^{-2}	$H_0 = 1$ Jm^{-1}nb^{-1}
$\beta = 7.04 \times 10^6$ Nm^{-2}deg^{-1}	$\tau = 5 \times 10^{-5}$ s
$\delta_n = -9 \times 10^{-31}$ m^{-3}	$N_0 = 10^{20}$ m^{-3},
$\rho = 2.33 \times 10^3$ K gm^{-3}	$\varepsilon_0 = 8.838 \times 10^{-12}$ Fm^{-1}
$C_e = 695$ J Kg^{-1}K^{-1}	$E_g = 1.11$ eV
$K = 150$ Wm^{-1}K^{-1}	$\alpha_T = 3 \times 10^{-6}$ K^{-1}
$K^* = 1.54 \times 10^2$ Ws	$s_v = 2$ ms^{-1}
$D_e = 2.5 \times 10^{-3}$ m^{2}s^{-1}	$H_0 = 10^8$ Col.cm^{-1}s^{-1}
$\mu_0 = 4\pi \times 10^{-7}$ Hm^{-1}	$\sigma_0 = 9.36 \times 10^5$ Col^{2}C^{-1}m^{-1}s^{-1}

A comparison of the dimensionless form of the field variables for a transversely isotropic plate with two temperature and frequency is demonstrated graphically as:

The dimensionless form of the field variables viz. components of displacement, thermodynamic temperature, conductive temperature, carrier density and axial stress as well as couple stress is visually represented as.

   i.   The black line relates to MGTPT with, $m = 0$,
   ii. The red line relates to MGTPT with, $m = 5$,
   iii. The purple line relates to MGTPT with, $m = 7$,
   iv. The green line relates to MGTPT with, $m = 10$,

Figure 2 illustrates the deviation in the displacement component u of the semiconducting sphere for MGTPT theory with Hall Effect. It has been noticed that in absence of Hall Effect under MGTPT theory, there is maximum variation in u. Though, in presence of Hall Effect, variation in the displacement is sharply decreases. Moreover, in the centre of the sphere, there is no variation in the displace component, but as radial distance increases, deviation in
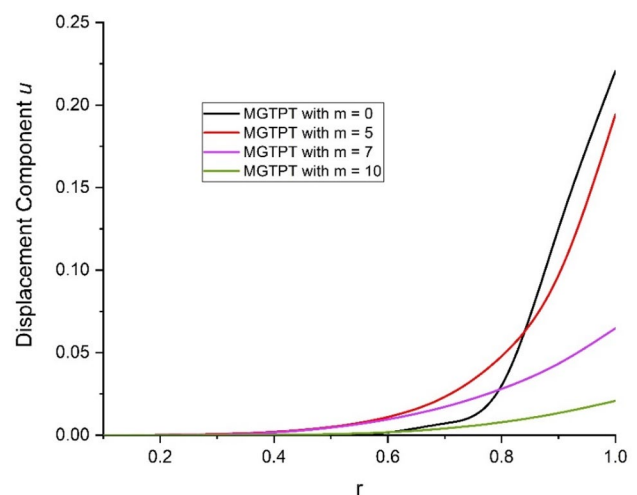

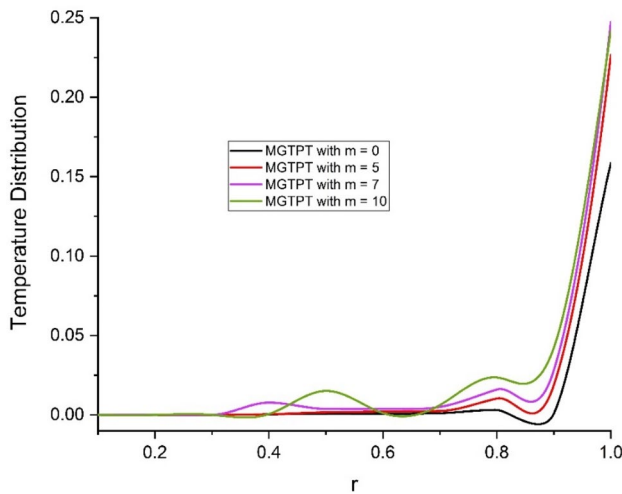**Fig. 2** The displacement deviation with Hall Effect under MGTPT

Fig. 3 The temperature deviation with Hall Effect under MGTPT
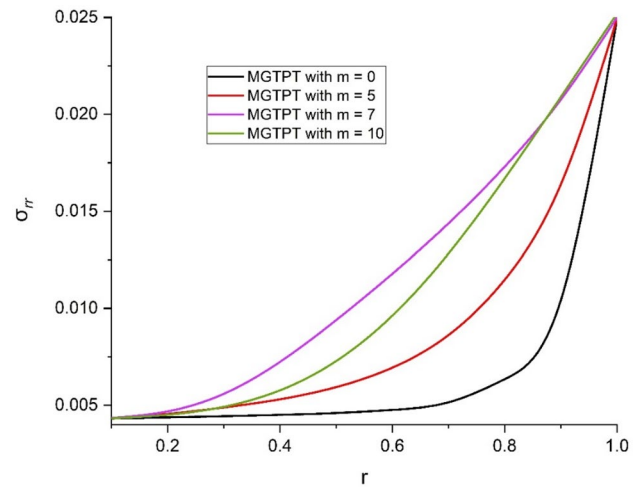

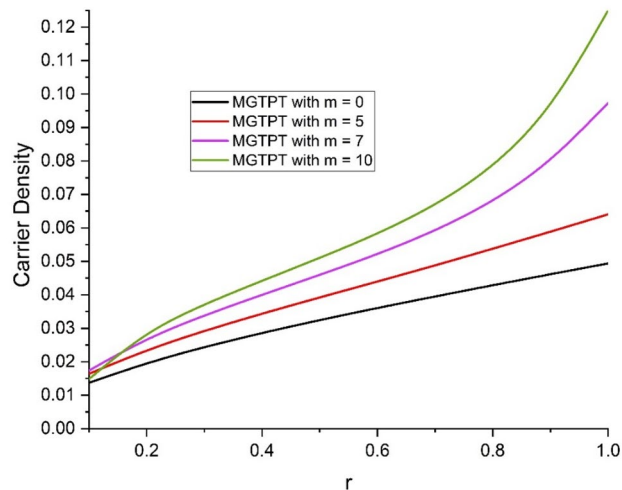**Fig. 5** The variation in radial stress with Hall Effect under MGTPT

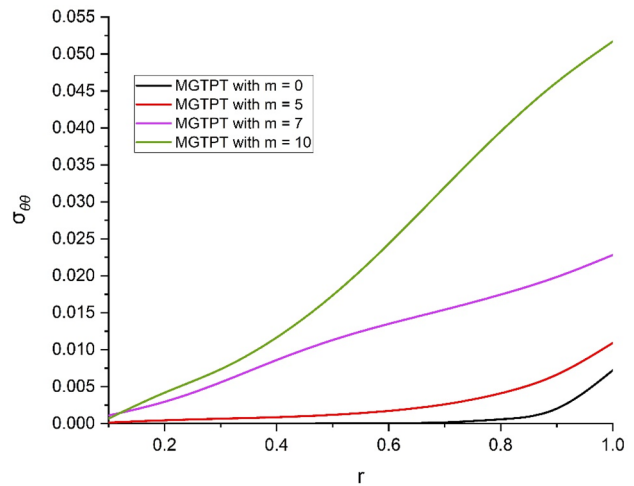**Fig. 4** The change in carrier density with Hall Effect under MGTPT

Fig. 6 The change in hoop stress with Hall Effect under MGTPT

the u increases sharply. Figure 3 demonstrates the deviation in the temperature distribution T in the semiconducting sphere with Hall Effect. It has been noticed that T is lesser in the inside core of the sphere as compared to the external core of the sphere. Additionally, presence of Hall Effect cause the higher variation in T.

Figure 4 shows the change in the carrier density in the semiconducting sphere for MGTPT theory with Hall Effect. It has been noticed that in absence of Hall Effect, the variation in carrier density is minimum. As soon as, Hall current increase, the carrier density sharply increases. In comparison to the sphere's outer core, the inner core's carrier density has been found to vary less. Figures 5, 6 shows the variation in the components of stress in the semiconducting sphere for MGTPT with Hall Effect. The radial stress in Fig. 5

illustrates that without Hall Effect with MGTPT theory, the variation are minimum. There is sharp change in the hoop stress as the Hall current increases. Furthermore, as compared to the outer core of the sphere, it has been observed that the inner core of the sphere experiences less variation in stress components.

Figure 7 illustrates the deviation in the displacement component u of the semiconducting sphere for various models. It has been observed that in absence of Hall Effect under PLS theory, there is maximum variation in u. Though, with MGTPT theory in presence of Hall Effect, variation in the displacement is sharply increases. Moreover, in the centre of the sphere, there is no variation in the displace component, but as radial distance increases, deviation in the u increases sharply. Figure 8 demonstrates the deviation in the temperature distribution T in the
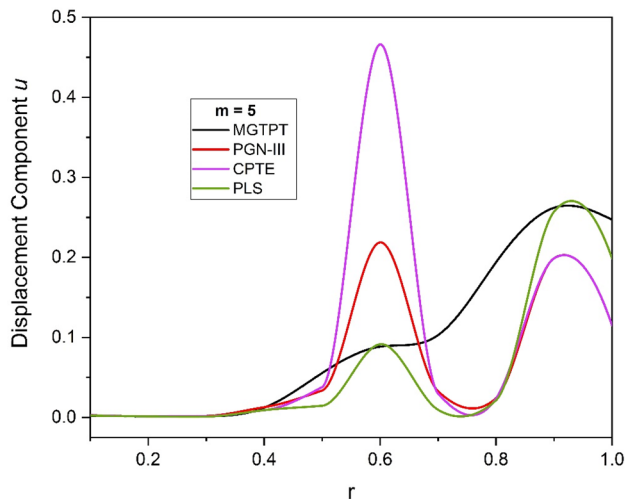
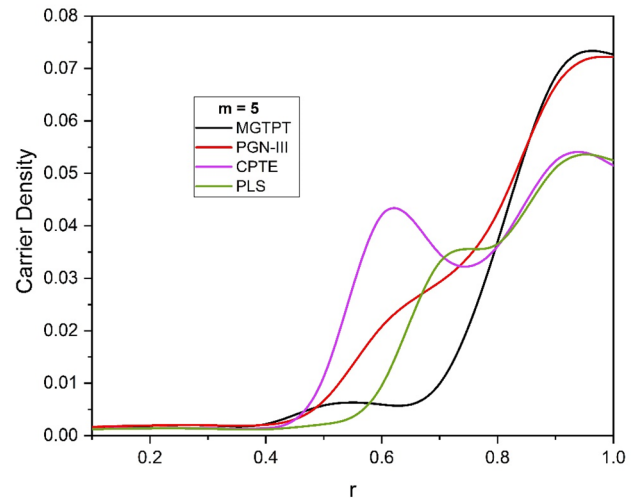**Fig. 7** The change of displacement for various models with Hall effect

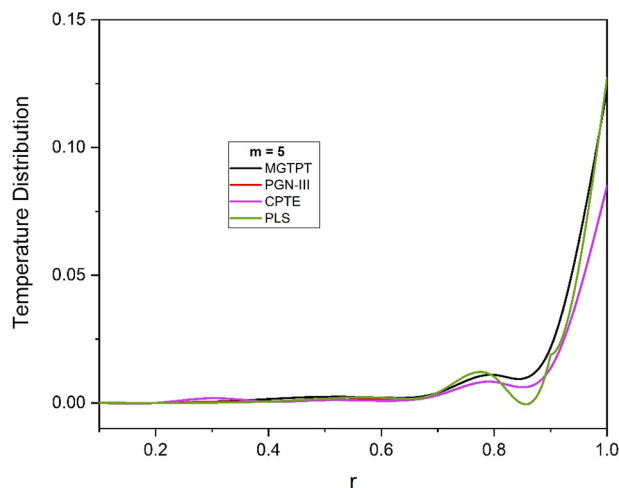**Fig. 9** The change in carrier density for different models

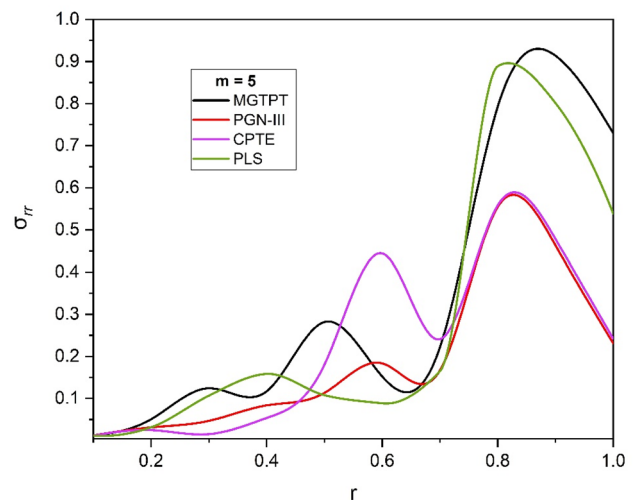**Fig. 8** The temperature change for different models

Fig. 10 The change in radial stress for different models

semiconducting sphere with various models. It has been noticed that T is lesser in the inside core of the sphere as compared to the external core of the sphere. Additionally, presence of Hall Effect cause the higher variation in T.

Figure 9 shows the change in the carrier density in the semiconducting sphere for various models with Hall Effect. It has been noticed that with MGTPT, the variation in carrier density is maximum and PLS shows the minimum variations in the carrier density. In comparison to the sphere's outer core, the inner core's carrier density has been found to vary less. Figures 10, 11 shows the variation

in the components of stress in the semiconducting sphere for various models with Hall Effect. The radial stress in Fig. 10 illustrates that MGTPT theory, the variation in radial stress is maximum whereas, hoop stress is minimum. There is sharp change in the hoop stress as the Hall current increases. However, PGN-III shows the minimum variation in radial stress and MGTPT illustrate maximum variation. Additionally, MGTPT shows the minimum variation in hoop stress and PLS illustrate maximum variation. Furthermore, as compared to the outer core of the sphere, it has been observed that the inner core of the sphere experiences less variation in stress components.
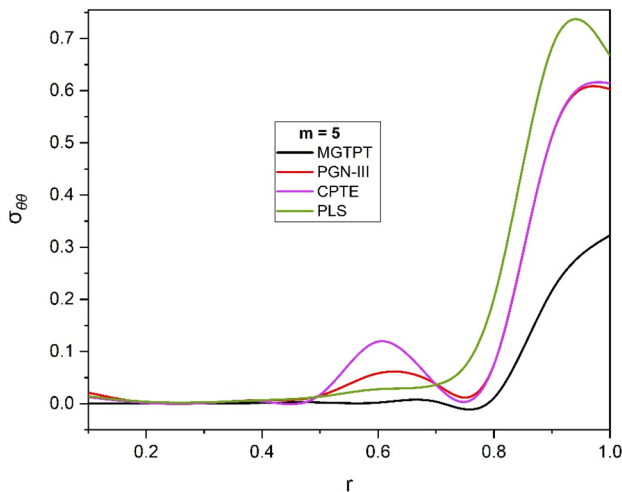
Fig. 11 The change in hoop stress with different models

8 Conclusions

- The rotating infinite semiconducting solid sphere has been investigated in this study under the influence of high magnetic field along its axis with the exponentially laser pulse applied on its boundary surface.

- The study is motivated not only by basic scientific interests, but also by the increasing need for faster interaction and information processing as well as the use of semiconductor optoelectronic and electronic devices. It is important to understand how semiconductors operate dynamically under Hall current effect so that microelectronic semiconductor devices may be improved. Hall Effect have an incredibly strong effect on the behavior of different distributions. In evaluating semiconducting materials, this should be taken into consideration, as the duration of the Hall current increases the carrier density and decreases the deviation in the displacement.

- It has been noticed that with MGTPT theory, the variation in radial stress is maximum whereas, hoop stress is minimum. However, PLS theory shows the higher variation in different components.

- The energy harvesting and generating the alternative energy sources is the need of the day. There is a significance contribution of the semiconductor materials to generate electrical energy from sunlight, even when subjected to laser light. The study may be helpful in designing of semiconductor nano-devices, Hall Effect sensors, magnetic switch, and applications in transistors, screens and solar cells as well as semiconductor nanostructure devices such as MEMS/NEMS.

Declarations

References

1. Duhamel JM (1938) Memories of the molecular actions developed by changes in temperatures in solids. Mummy Div Sav (AcadSci Par) 5:440–498
2. Biot MA (1956) Thermoelasticity and irreversible thermodynamics. J Appl Phys 27:240–253. https://doi.org/10.1063/1.1722351
3. Cattaneo C (1958) A form of heat-conduction equations which eliminates the paradox of instantaneous propagation. C R Acad Sci Paris Ser II 247:431–433
4. Vernotte P (1958) Les paradoxes de la theorie continue de l'equation de lachaleur. C R Acad Sci Paris Ser II 246:3154–3155
5. Vernotte P (1961) Some possible complications in the phenomena of thermal conduction. C R Acad Sci Paris Ser II 252:2190–2191
6. Lord HW, Shulman Y (1967) A generalized dynamical theory of thermoelasticity. J Mech Phys Solids 15:299–309. https://doi.org/10.1016/0022-5096(67)90024-5
7. Green AE, Lindsay KA (1972) Thermoelasticity. J Elast 2:1–7. https://doi.org/10.1007/BF00045689
8. Dhaliwal RS, Sheriff HH (1980) Generalized thermoelasticity for anisotropic media. Q Appl Math 38:1–8
9. Green AE, Naghdi PM (1991) A re-examination of the basic postulates of thermomechanics. Proc R Soc Lond Ser A Math Phys Sci 432:171–194. https://doi.org/10.1098/rspa.1991.0012

10. Green AE, Naghdi PM (1992) On undamped heat waves in an elastic solid. J Therm Stress 15:253–264. https://doi.org/10.1080/01495739208946136

11. Green AE, Naghdi PM (1993) Thermoelasticity without energy dissipation. J Elast 31:189–208. https://doi.org/10.1007/BF00044969

12. Lasiecka I, Wang X (2015) Moore-Gibson-Thompson equation with memory, part II: general decay of energy. Anal PDEs. https://doi.org/10.48550/arXiv.1505.07525

13. Quintanilla R (2019) Moore–Gibson–Thompson thermoelasticity. Math Mech Solids 24:4020–4031. https://doi.org/10.1177/1081286519862007

14. Quintanilla R (2020) Moore-Gibson-Thompson thermoelasticity with two temperatures. Appl Eng Sci 1:100006. https://doi.org/10.1016/j.apples.2020.100006

15. Fernández JR, Quintanilla R (2021) Moore-Gibson-Thompson theory for thermoelastic dielectrics. Appl Math Mech 42:309–316. https://doi.org/10.1007/S10483-021-2703-9

16. Kaur I, Singh K, Craciun E-M (2022) A mathematical study of a semiconducting thermoelastic rotating solid cylinder with modified Moore–Gibson–Thompson heat transfer under the hall effect. Mathematics 10:2386. https://doi.org/10.3390/math10142386

17. Gupta S, Das S, Dutta R (2020) Influence of gravity, magnetic field, and thermal shock on mechanically loaded rotating FGDPTM structure under Green-Naghdi theory. Mech Based Des Struct Mach. https://doi.org/10.1080/15397734.2020.1853565

18. Gupta S, Das S, Dutta R, Verma AK (2022) Higher-order fractional and memory response in nonlocal double poro-magneto-thermoelastic medium with temperature-dependent properties excited by laser pulse. J Ocean Eng Sci. https://doi.org/10.1016/j.joes.2022.04.013

19. Gupta S, Dutta R, Das S (2022) Memory response in a nonlocal micropolar double porous thermoelastic medium with variable conductivity under Moore-Gibson-Thompson thermoelasticity theory. J Ocean Eng Sci. https://doi.org/10.1016/j.joes.2022.01.010

20. Craciun EM, Baesu E, Soós E (2005) General solution in terms of complex potentials for incremental antiplane states in pre-stressed and prepolarized piezoelectric crystals: application to mode III fracture propagation. IMA J Appl Math (Inst Math Appl) 70:39–52. https://doi.org/10.1093/IMAMAT/HXH060

21. Craciun E-M, Baesu E, Soós E (2004) General solution in terms of complex potentials for incremental antiplane states in pre-stressed and prepolarized piezoelectric crystals: application to Mode III fracture propagation. IMA J Appl Math 70:39–52. https://doi.org/10.1093/imamat/hxh060

22. Kaur I, Singh K (2021) Fractional order strain analysis in thick circular plate subjected to hyperbolic two temperature. Partial Differ Equ Appl Math 4:100130. https://doi.org/10.1016/J.PADIFF.2021.100130

23. Kaur I, Singh K (2021) Plane wave in non-local semiconducting rotating media with Hall effect and three-phase lag fractional order heat transfer. Int J Mech Mater Eng 16:1–16. https://doi.org/10.1186/S40712-021-00137-3/FIGURES/16

24. Kaur I, Lata P, Singh K (2021) Study of transversely isotropic non-local thermoelastic thin nano-beam resonators with multi-dual-phase-lag theory. Arch Appl Mech 91:317–341. https://doi.org/10.1007/s00419-020-01771-7

25. Tiwari R, Mukhopadhyay S (2017) On electromagneto-thermoelastic plane waves under Green-Naghdi theory of thermoelasticity-II. J Therm Stress 40:1040–1062. https://doi.org/10.1080/01495739.2017.1307094

26. Kaur I, Lata P, Singh K (2020) Effect of Hall current in transversely isotropic magneto-thermoelastic rotating medium with fractional-order generalized heat transfer due to ramp-type heat. Indian J Phys. https://doi.org/10.1007/s12648-020-01718-2

27. Tiwari R, Kumar R, Abouelregal AE (2022) Thermoelastic vibrations of nano-beam with varying axial load and ramp type heating under the purview of Moore–Gibson–Thompson generalized theory of thermoelasticity. Appl Phys A 128:160. https://doi.org/10.1007/s00339-022-05287-5

28. Tiwari R, Misra JC, Prasad R (2021) Magneto-thermoelastic wave propagation in a finitely conducting medium: a comparative study for three types of thermoelasticity I, II, and III. J Therm Stress 44:785–806. https://doi.org/10.1080/01495739.2021.1918594

29. Marin M, Othman MIA, Seadawy AR, Carstea C (2020) A domain of influence in the Moore–Gibson–Thompson theory of dipolar bodies. J Taibah Univ Sci 14:653–660. https://doi.org/10.1080/16583655.2020.1763664

30. Gupta S, Dutta R, Das S, Pandit DK (2022) Hall current effect in double poro-thermoelastic material with fractional-order Moore–Gibson–Thompson heat equation subjected to Eringen's nonlocal theory. Waves Random Complex Media. https://doi.org/10.1080/17455030.2021.2021315

31. Gupta S, Das S, Dutta R (2021) Peltier and Seebeck effects on a nonlocal couple stress double porous thermoelastic diffusive material under memory-dependent Moore-Gibson-Thompson theory. Mech Adv Mater Struct. https://doi.org/10.1080/15376494.2021.2017525

32. Kumar R, Tiwari R, Singhal A (2022) Analysis of the photo-thermal excitation in a semiconducting medium under the purview of DPL theory involving non-local effect. Meccanica 57:2027–2041. https://doi.org/10.1007/s11012-022-01536-2

33. Mahdy AMS, Lotfy K, Ahmed MH, El-Bary A, Ismail EA (2020) Electromagnetic Hall current effect and fractional heat order for microtemperature photo-excited semiconductor medium with laser pulses. Results Phys 17:103161. https://doi.org/10.1016/j.rinp.2020.103161

34. Abouelregal AE, Atta D (2022) A rigid cylinder of a thermoelastic magnetic semiconductor material based on the generalized Moore–Gibson–Thompson heat equation model. Appl Phys A 128:118. https://doi.org/10.1007/s00339-021-05240-y

35. Press WH, Teukolsky SA, Flannery BP (1980) Numerical recipes in Fortran. Cambridge University Press, Cambridge